Nanoscale

RSC Publishing

FEATURE ARTICLE

View Article Online
View Journal | View Issue

Cite this: *Nanoscale*, 2013, **5**, 2589

Design and applications of gold nanoparticle conjugates by exploiting biomolecule–gold nanoparticle interactions

Shao Su,[a] Xiaolei Zuo,[b] Dun Pan,[b] Hao Pei,[b] Lianhui Wang,*[a] Chunhai Fan*[b] and Wei Huang[a]

Received 29th November 2012
Accepted 3rd January 2013

DOI: 10.1039/c3nr33870c

www.rsc.org/nanoscale

Gold nanoparticles (AuNPs) are a type of widely used nanomaterials with unique chemical and physical properties. AuNPs can be readily synthesized, and modified with various chemical or biological molecules, making them promising candidates for catalysis, drug delivery and biological imaging applications. In this review, we mainly focus on recent advances in the design and synthesis of conjugates of AuNPs by exploiting biomolecule–AuNP interactions. We will also discuss a variety of bioapplications of AuNP-based conjugates.

1 Introduction

Gold nanoparticles (AuNPs), as one of the most investigated nanomaterials, possess unique chemical and physical properties, such as size- and shape-dependent optical and electronic features, high surface-to-volume ratio, excellent biocompatibility and chemical stability. Hence, AuNPs have fascinated scientists for over a century, and have been widely employed in the assembly of ordered nanostructures,[1,2] catalysis,[3,4] sensors,[5–7] drug delivery,[8–10] biological imaging,[11] therapy[12] and so on.

In 1996, both the Mirkin group and the Alivisatos group reported the synthesis of a DNA–AuNPs conjugate, which opened up an exciting AuNPs-based bionanotechnology field.[13,14] Following their pioneering work, more-and-more researchers focused on AuNPs as biological nanoprobes in bionanotechnological applications. AuNPs are easily functionalized with ligands such as DNA, proteins, and antibodies *via* Au–S, or Au–N covalent bonds. or Au–protein or Au–antibody interactions, which result in a broad range of applications. Since there have been excellent reviews on applications of AuNPs-based conjugates for drug/siRNA delivery,[8,15] biodetection[5,6] and biomedicine,[9,10,16] we will focus on overviews of

[a]*Key Laboratory for Organic Electronics & Information Displays (KLOEID), Institute of Advanced Materials (IAM), School of Materials Science and Engineering, Nanjing University of Posts & Telecommunications, 9 Wenyuan Road, Nanjing, 210046, China*
[b]*Laboratory of Physical Biology, Shanghai Institute of Applied Physics, Chinese Academy of Sciences, Shanghai 201800, China. E-mail: fchh@sinap.ac.cn*

Shao Su received his BS degree from Anhui Normal University in 2007, and then he moved to Shanghai Institute of Applied Physics (SINAP), Chinese Academy of Sciences as a PhD student and received his PhD degree in 2010. After two years of postdoctoral research at the SINAP, he became a lecturer in School of Materials Science and Engineering, Nanjing University of Post & Telecommunications in 2012. His research interests focus on electrochemical and optical biosensors based on different nanomaterials.

Lianhui Wang graduated from Fujian Normal University with a MS degree in 1993. Then he received his PhD degree from Zhejiang University in 1998. After working at the National University of Singapore for seven years, he joined Fudan University as a professor in 2005. In 2011, he moved to Nanjing University of Post & Telecommunications as a chair professor. His research interests include nanobiology, chemical biology, bioelectronics, biosensors and so on. He has published over 100 papers in international, peer-reviewed journals, the citations of which exceed 2500 giving him an h-index of 27.

recent advances in biomolecule–AuNP conjugates during the last several years.

2 Conjugation of ligand-protected gold nanoparticles

Ligand-protected AuNPs (citrates, thiols and amine ligands) can be easily obtained by chemical synthesis and ligand exchange reactions. A classic approach to the synthesis of AuNPs uses the reduction of $HAuCl_4$ by citrate, where the citric acid acts as both the reducing agent and stabilizer.[17] Unfortunately, citrate-capping AuNPs are not stable under severe conditions, such as high salt or metal ions, limiting their further bioapplication. Therefore, to enlarge AuNP application, many researchers are devoted to explore and synthesize stable ligand-protected AuNPs.

For many applications, it is desirable to stabilize the colloids over a wide range of buffer conditions while still retaining surface accessibility for adsorption and reaction. Based on their previous studies,[18] Liu's group have explored the stability of AuNPs in a diverse range of buffer conditions using polyethylene glycol (PEG) as the depletion agent.[19] They found AuNPs can be easily aggregated in the presence of low molecular weight PEG with a red-to-blue color change. However, if they used high molecular weight PEG as depletion agent, AuNPs would have ultrahigh stability at extremely high ionic strength or extreme pH (pH 1–13), as well as in the presence of heavy metal ions, organic solvents and small molecule adsorbates, while still retaining surface accessibility (Fig. 1). Consistent with theoretical study, they also propose that depletion stabilization is a function of PEG size.

2.1 Specific interactions of DNA–gold nanoparticles

2.1.1 Interactions through Au–S bonds. Following the pioneering work of Mirkin *et al.*[14] and Alivisatos *et al.*,[13] it has become a popular method to obtain stable and functionalized AuNPs *via* Au–S bonds.[20] The thiol-protected AuNPs usually have a high DNA monolayer density, which are extremely stable even in very high ionic solutions (*e.g.*, >1 M NaCl). For example, Kanehare and coworkers reported the size control of the thiol-protected AuNPs assisted by proton acids and halogen anions under mild conditions at room temperature.[21] Mirkin's group systematically explored the factors influencing the reaction between thiol-terminated oligonucleotides and AuNPs.[22,23] Classic thiolated DNA is conjugated on AuNPs and NaCl is gradually added to increase DNA loading over 1–2 days. Zhang *et al.* developed a fast method using a citrate buffer in pH 3.0 to complete the thiolated DNA attachment process in a few minutes.[24] As shown in Fig. 2, two tubes of solution each containing 10 nM of citrate-capped AuNPs were mixed with 3 μM thiolated DNA in the buffer of pH 7.6 and 3.0, respectively. After 3 min, NaCl was added. The sample at pH 7.6 immediately turned purple, indicating AuNP aggregation, but that at pH 3.0 remained red. The sample was then centrifuged and redispersed in DNA hybridization buffer. The sample of pH 7.6 turned blue right away, while that of pH 3.0 remained red even at 1 M NaCl (Fig. 2D).

It is important to not only maintain a stable linkage between AuNPs and DNA, but also maintain the stability during the purification process of DNA–AuNPs conjugates for subsequent applications. However, such a bond is susceptible to oxidation in air and water, resulting in compromised long-term stability.[20] Recently, Bhatt *et al.* focused on studying the Au–S bond dissociated at high salt, high pH, and high temperature, little DNA degraded even under such severe conditions.[25] Most organic solvents, however, showed a moderate protection effect on the Au–S bond. According to their results, they suggested the purified DNA-functionalized AuNPs should be freshly prepared and used in a day or two. Long-term storage should be carried out at relatively low temperature in low salt and slightly acidic buffers.

2.1.2 Interactions through Au–polyA. It is still a critical challenge to control reproducible DNA surface density on the gold surface. The surface density of thiolated DNA on AuNPs

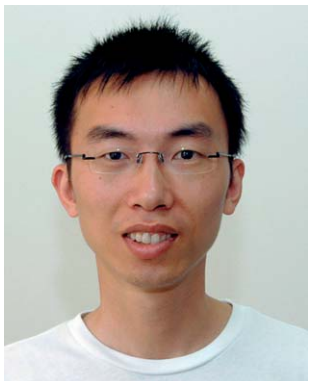

Chunhai Fan obtained his BS and PhD from the Department of Biochemistry at Nanjing University in 1996 and 2000. After his postdoctoral research at University of California, Santa Barbara, he joined the faculty at Shanghai Institute of Applied Physics (SINAP), Chinese Academy of Sciences (CAS) in 2004. He is now Professor and Chief of the Division of Physical Biology at SINAP. He is also the associate editor of ACS Applied Materials & Interfaces. He has published over 200 papers in peer-reviewed journals. His research interests focus on DNA nanotechnology, biosensors and biophotonics.

Wei Huang received his bachelor degree (1982) in chemistry from Peking University (China), and continued with graduate study (Master and Doctor) and working as a teacher in Peking University. He moved to National University of Singapore and worked as a postdoc research associate in 1993. He joined Fudan University as a professor in 2001. In 2006, he moved to Nanjing University of Post & Telecommunications as a chair professor. He has been an Academician of the Chinese Academy of Sciences since 2011. His research interests focus on organic optoelectronics, information display and photoelectric technology and nanomaterials.

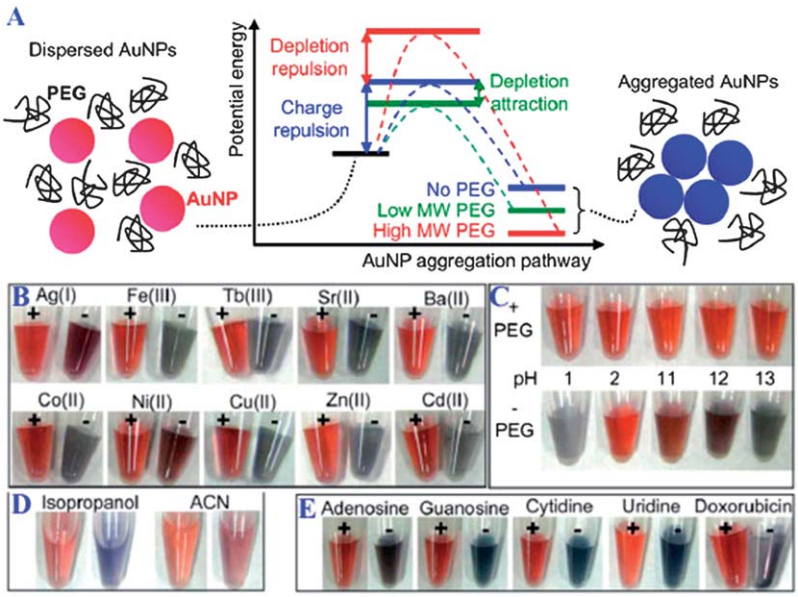

Fig. 1 (A) Schematics of the potential energy diagram of AuNP aggregation (not to scale). Effect of 2% PEG 20 000 on the stability of citrate-capped 13 nm AuNPs in the presence of (B) various heavy metal ions: 4 mM Ba^{2+}, 10 mM Sr^{2+}, and 2 mM for the rest, (C) buffer pH, (D) 67% organic solvents and (E) ribonucleosides (A = 5 μM, G = 0.25 mM, C = 2 mM, U = 20 mM) and doxorubicin (2 μg mL^{-1}). Reprinted from ref. 19 with the permission of the American Chemical Society.

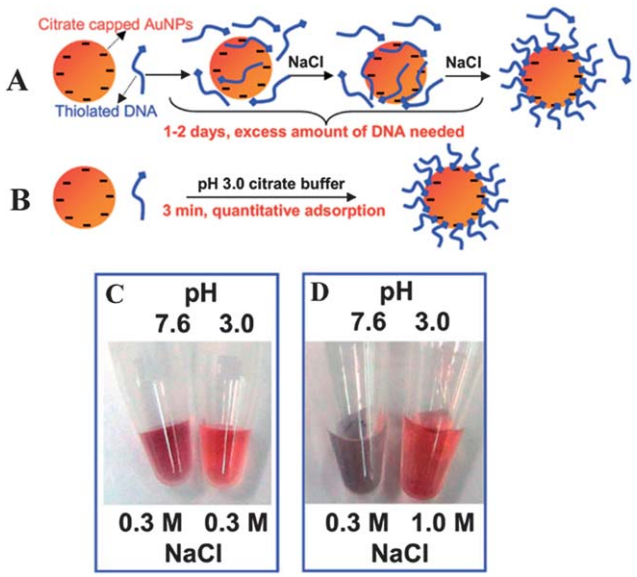

Fig. 2 Schematics of attaching negatively charged thiolated DNA to negatively charged AuNPs using salt aging (A) and low pH assisted (B) methods. (C) Photograph of AuNPs mixed with DNA for 3 min at pH 7.6 or 3.0 followed by adding 0.3 M NaCl. (D) The samples were prepared the same way as in (C), but the free DNA was removed, and AuNPs were redispersed in buffers containing 0.3 M NaCl and pH 7.6 or 1.0 M NaCl and pH 7.6. Reprinted from ref. 24 with the permission of the American Chemical Society.

can be controlled by post-treating DNA-coated surfaces with displacing small thiols. However, the kinetics of the displacement reaction vary with the solution and surface conditions, limiting the reproducibility. Therefore, many researchers have focused on exploring the native properties of DNA bases. Previous studies have shown that DNA bases chemisorbed on gold surface in the order of G > A > C > T.[26] Moreover, polyadenine (polyA) sequences containing multiple consecutive adenines preferentially adsorb gold surface with high affinity, even comparable to Au–S chemistry. Opdahl and coworkers observed that the grafting density and conformation of single-stranded DNA brushes were deterministically controlled by the length of the anchoring dA sequences.[27] On the basis of previous works, they have systematically studied the interaction of dA and the gold surface.[28,29] More recently, we have designed a new strategy for modification-free, diblock DNA oligonucleotides and rapid hybridization in colorimetric DNA detection with plasmonic conjugates.[30] Interestingly, the diblock oligonucleotide-based conjugates showed many advantageous over faster hybridization kinetics than thiol–DNA conjugates and more convenient and controllable than the previously reported method with the displacement reagent 6-mercapto-1-heanol (MCH). The article also pointed out that polyA not only offers the anchoring function but also effectively blocks nonspecific DNA–Au binding, providing a reproducible and well-defined surface density and favorable hybridization ability (Fig. 3).

2.2 Non-specific interactions of ligand–gold nanoparticles

2.2.1 Au–N bonds. Well-established Au–S chemistry has proven powerful in the self-assembly of biomolecules on the surface of AuNPs. For the purpose of biological applications (such as controlled drug-releasing systems), Au–N bonds are considered as the ideal model for constructing AuNPs-based conjugates.[31] For example, Tang and coworkers developed three-dimensional AuNPs-decorated amine-terminated poly(amidoamine) dendrimers for sensitive electrochemical immunoassay of brevetoxins in food samples *via* Au–N bond.[32] More importantly, the effect of ligands possessing both amine

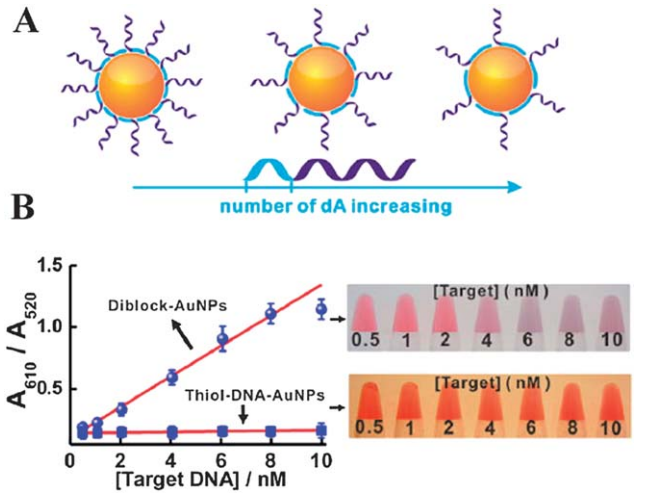

Fig. 3 (A) Schematic for spatial control on AuNPs by varying the length of polyA blocks. (B) Dose–response curves and photographic images for DNA detection by using two types of conjugates (in 10 min). Reprinted from ref. 30 with the permission of the American Chemical Society.

and thiol groups on the surface of AuNPs were investigated. Aina *et al.* demonstrated that AuNPs can be selectively functionalized with small molecules carrying either amino or thiol groups by simply varying the temperature and pH.[33] They found it is possible to obtain a strong Au–S bond, whereas at room temperature, a weak Au–N linkage is formed in the presence of cysteine and cystine at pH = 9. More recently, Chegel and coworkers have experimentally and theoretically investigated the effect of amino or thiol groups on the surface of AuNPs using spectrophotometry of the localized surface plasmon resonance (LSPR) and finite-difference time-domain (FDTD) modeling.[34] They found that the compound (like aminomethane and ethanol amine) containing amine group(s) but the lack of a sulfur atom also can efficiently stabilize colloidal AuNPs at low concentrations. By adding a high concentration of the compound (3 mM), a strong decrease in peak intensity at 520 nm with the concurrent appearance of a broad peak in the range 650–700 nm was obtained. They speculated that the compound probably forms a diffuse layer near the AuNPs' surface without replacement of citrate ions and only partially neutralizes their negative charge. They also found that organic compounds containing both thiol and amine groups strongly promote the aggregation of AuNPs due to their cooperative functionalities.

2.2.2 Au–C bond. The above-described covalent bonds of Au–S, Au–poly A, and Au–N have been successfully employed in ligand-protected AuNPs, but what about other covalently bonds? Indeed, it is possible to form Au–C bonds on the gold surface. Several groups have reported on the formation of aryl films on a gold surface *via* the reduction of diazonium salts.[35,36] However, there is still a lack of direct evidence for Au–C covalent bonds. Previously, McDermott's group has shown that diazonium-derived nitrobenzene films are more strongly bonded to gold surfaces than the thiol analogue.[37] More recently, they offered direct evidence for diazonium-derived aryl films on AuNPs *via* an Au–C bond characterized by surface-enhanced Raman scattering and high-resolution electron energy loss spectra.[38] The useful evidences may benefit further AuNPs-based applications.

3 Applications of AuNP-based conjugates

3.1 Biosensing

The detection of chemical and biological molecules plays a vital role in biomedical diagnostics, food safety, environmental monitoring, forensic analysis and anti-bioterrorism. AuNPs possess unique physicochemical properties that offer a suitable platform for constructing new recognition and transduction processes for chemical and biological sensors. In the past decades, AuNPs-based sensors have been successfully applied in the detection of DNA,[6,39,40] proteins,[40–42] various virus sequences (such as influenza A (H1N1),[43] hepatitis C[44]), metal ions[45–47] and these sensors are highly sensitive and selective, cost-effective, and miniaturised.

Aptamer-conjugated AuNPs that combine the selectivity and affinity of aptamers with the unique properties of AuNPs were utilized to detect small molecules and cancer cells.[48,49] Zhang *et al.* have combined the highly specific binding abilities of aptamers with the ultrahigh quenching ability of AuNPs to develop a novel aptamer-based multicolor nanoprobe for multiplex detection of adenosine, potassium and cocaine in homogeneous solutions (Fig. 4).[48] Moreover, the different analogue molecules (negative control) only caused minimal fluorescence increase.

Recently, colloidal AuNPs were found to exhibit glucose oxidase-like activity.[50,51] More recently, we designed a self-limiting growth system based on the fact that the enzyme-like

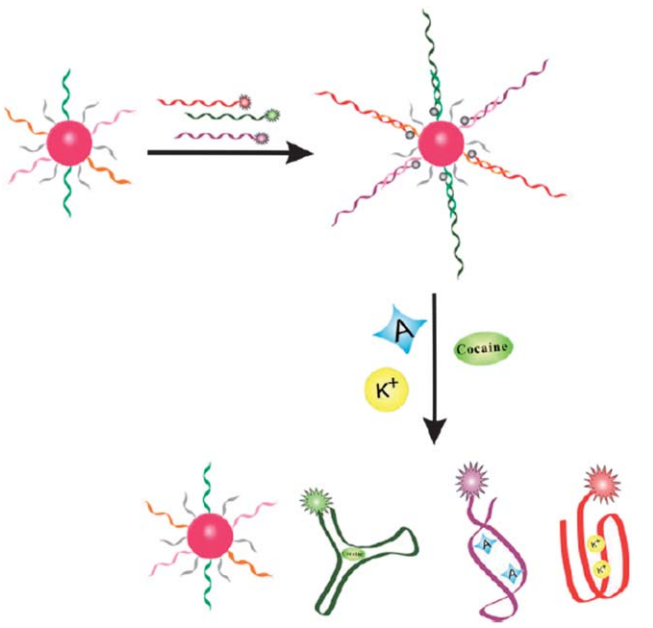

Fig. 4 A multicolor aptamer-based gold nanoprobe for the multiplex detection of adenosine (A), potassium, and cocaine. Reprinted from ref. 48 with the permission of Wiley-VCH.

activity of AuNPs was extremely sensitive to surface properties.[51] On the basis of previous work, Zheng *et al.* utilized catalytic AuNPs as a nanoplasmonic probe for biomolecular detection.[52] They amplified the noncovalent ability for single-stranded (ss-) DNA to bind nanocovalently AuNPs much more rapidly and strongly than to double-stranded (ds-) DNA. The AuNPs-based nanoplasmonic probe successfully accomplished multiple-analyte detection, such as DNA, microRNAs, and K^+. Moreover, the ss-DNA–AuNPs-seeded and ds-DNA–AuNPs-seeded growth processes were real-time monitored by dark-field microscopy (DFM), as shown in Fig. 5.

In addition to classic chemical and biological sensing, AuNPs-based sensors are also used in cells,[53,54] bacteria detection[55] and glucose detection in rat brain.[56] Rotello's group reported a colorimetric enzyme–AuNPs conjugate biosensor that used enzyme amplification to provide high sensitivity for the detection of pathogens in aqueous solutions.[55] Cationic AuNPs as enzyme inhibitors are electrostatically bound to β-galactosidase (β-Gal), inhibiting enzyme activity. Once bacteria bind to the AuNPs, β-Gal is released from the AuNPs and restores its activity, providing an enzyme-amplified colorimetric readout of the binding event. Using this strategy, the sensor can quantify bacteria as low as 100 cells per mL in solution.

3.2 Drug delivery and therapy

To achieve the purpose of tumor therapeutics, it is necessary to deliver as many as anti-cancer drugs to the tumor as is possible, and to control the release of drugs. Conventional tumor therapies (surgery, chemotherapy and radiation therapy) have been practised for decades, but they have their drawbacks, including low specificity for recognizing cancer cells and normal cells, and can be greatly harmful to the human body. Therefore, it is a critical challenge to improve the specificity and decrease the side effects of cancer therapy. With the development of nanotechnology, nanomaterials show great potential in applications of cancer therapy, such as AuNPs, Fe_3O_4,[57,58] and carbon nanotubes.[59,60] Among these nanomaterials, AuNPs have been considered as valuable nanocarriers for delivering anti-cancer drugs (such as doxorubicin,[61,62] oxaliplatin[63]) or siRNA[15] to specific sites of tumor cells.

First of all, it is necessary to improve the efficiency of anticancer drug delivery. AuNPs have been considered as drug delivery vehicles because they are essentially inert, high surface-to-volume ratio, non-toxic, biocompatible and easily decorated with specific molecules (such as small drug molecules) *via* different covalent bonds. AuNPs-based nanocarriers effectively deliver anticancer drugs into tumour cells through passive or active target mechanisms. Passive targets take advantage of the inherent size of AuNPs and the unique properties of tumour vasculature, such as enhanced permeability and retention (EPR) effects. As we know, AuNPs accumulate inside tumour tissues due to their defective vascular architecture coupled with poor lymphatic drainage.[64] AuNPs-based nanocarriers can provide efficient delivery of siRNA and drugs to tumour sites *via* the EPR effect.[65–67] Anticancer drugs accumulate in the tumour sites at usually 10-fold or greater when delivered by AuNPs compared to the free drug. Unfortunately, the accumulation of AuNPs in tumours depends on the size, surface characteristics and circulation half-life of the AuNPs, which further limits their applications. To overcome the limitations (low therapeutic and imaging efficiency) of passive targets, an alternative strategy (active targets) is developed by conjugating targeting moieties, such as peptides,[68] aptmers[8] or antibodies[69] to AuNPs. For example, Kim *et al.* chose multicellular tumour cylindroids as an *in vitro* tumour model to monitor systematically extracellular diffusion, cellular uptake and molecular release from AuNPs in real time (Fig. 6).[70] AuNPs carrying either fluorescein or doxorubicin molecules move and localize to different tumor tissues, depending on whether the nanoparticles are positively or negatively charged. The experimental results indicate that uptake is the dominant mechanism in particle delivery and the surface charges of AuNPs can control tissue penetration and drug release, which may overcome some of the current limitations in drug delivery. Besides, Rotello[71] and Ashley's[72] groups also have both reported an AuNP-based drug delivery system.

Another challenge is the specificity of drug delivery, which greatly enhances the effect of the cancer drugs. DNA and antibodies can locate to specific sites of cancer cells, and have been successfully employed in cancer treatment. Controlled AuNPs have been easily synthesized with tunable surface functionalities and have great potential for accumulation and specific locations at tumor sites. Duan's group has reported a multifunctional nanocarrier for anticancer drugs and plasmonic

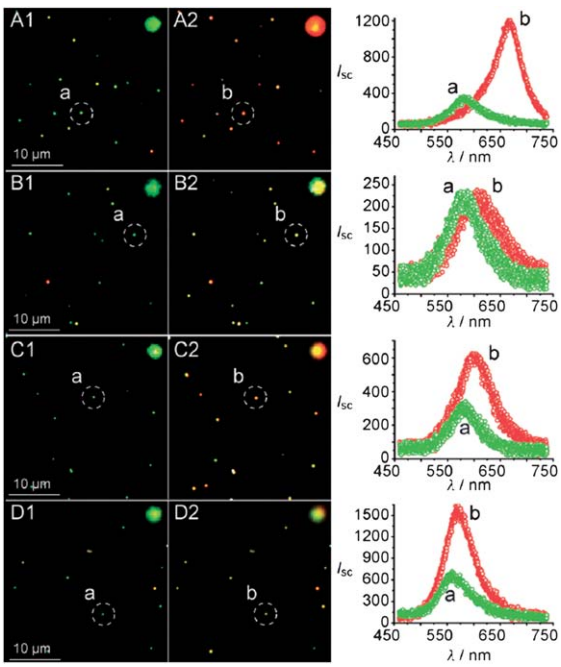

Fig. 5 Left: dark-field microscopy (DFM) images of large AuNPs (50 nm in diameter) before (1) and after (2) the 25 min glucose-induced enlargement process. (A) Bare AuNPs, (B) ss-DNA–AuNPs, (C) ds-DNA–AuNPs and (D) ds-DNA with 1-base mismatches interacting with AuNPs. Right: the light scattering spectra corresponding to individual nanoparticle marked with the circle in the DFM images. I_{sc} = scattering intensity. Reprinted from ref. 52 with the permission of Wiley-VCH.

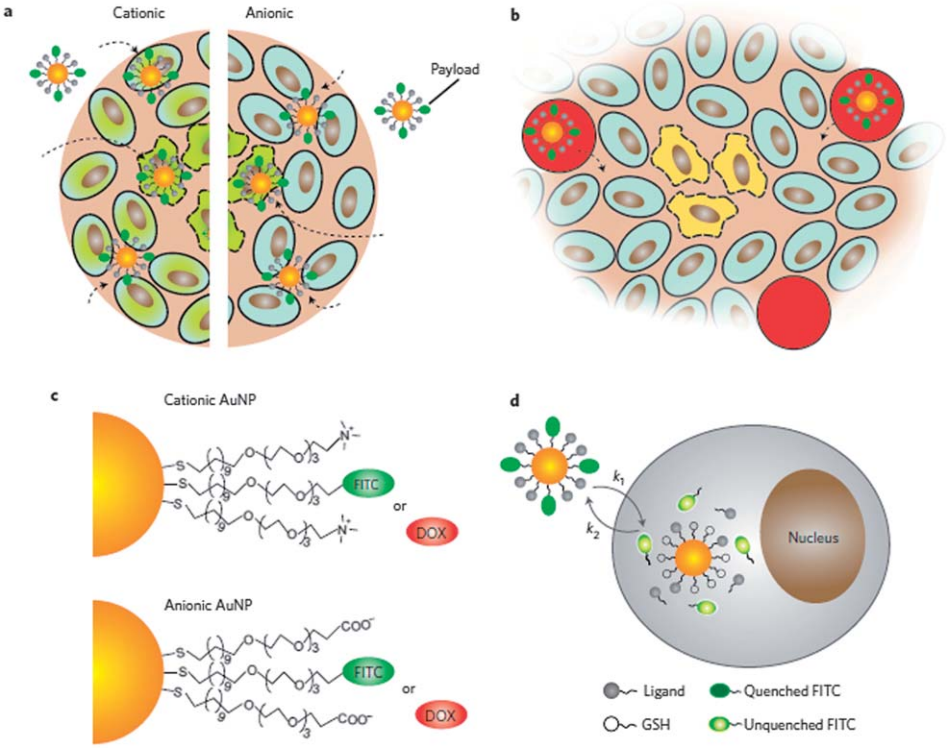

Fig. 6 Schematic showing the delivery of payload by gold nanoparticles. (a) Delivery of payload (green ovals) into tumour cylindroids by gold nanoparticles (gold circles). Cells containing released FITC–SH are in green. Viable cells are shown with smooth, solid boundaries, and necrotic cells have irregular, dashed boundaries. Dashed arrows indicate diffusion and cellular uptake. In cylindroids, nanoparticles are present in the medium outside the boundary of the cell mass. (b) Intratumoral delivery by gold nanoparticles following extravasation from the vessel lumen (red circles). (c) Mixed monolayer-protected gold nanoparticles loaded with thioalkylated FITC or doxorubicin (DOX). (d) Cellular uptake and FITC–SH release by thiol-mediated replacement reactions. Reprinted from ref. 70 with the permission of Nature Publishing Group.

imaging probes to label specifically targeted cancer cells.[73] Amphiphilic AuNPs carrying mixed polymer brushes with functional AuNPs embedded in the shell formed by the hydrophobic brushes, and the hydrophilic brushes extending into the aqueous environment to stabilize the structures, are illustrated in Fig. 7. They utilized the surface-enhanced Raman scattering (SERS) *in vivo* imaging technique, which can directly ascertain whether the AuNPs-based nanocarriers bind to the tumor sites or not. More interestingly, pH-responsive disassembly of the plasmonic vesicle, stimulated by the hydrophobic-to-hydrophilic transition of the hydrophobic brushes in acidic intracellular compartments, allows for triggered intracellular drug release, which can also be monitored in real-time by both plasmonic imaging and Raman spectroscopy.[73]

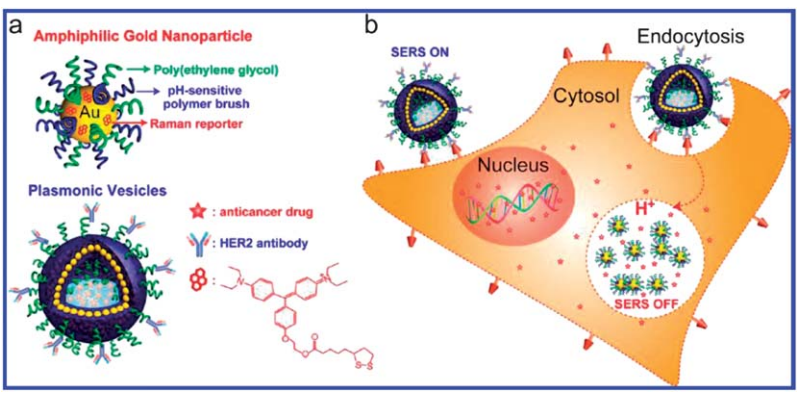

Fig. 7 (a) Schematic illustration of the amphiphilic gold nanoparticle coated with Raman reporter BGLA and mixed polymer brushes of hydrophilic PEG and pH-sensitive hydrophobic PMMAVP grafts and the drug-loaded plasmonic vesicle tagged with HER2 antibody for cancer cell targeting. (b) The cellular binding, uptake, and intraorganelle disruption of the SERS-encoded pH-sensitive plasmonic vesicles. Reprinted from ref. 73 with the permission of the American Chemical Society.

Controlled drug release is a vital adjunct for biomedical implants and targeted drug delivery systems. The ease of incorporation of drugs and biomolecules coupled with low fabrication costs makes electrostatic layer-by-layer (LBL) assembly a versatile technique for controlled release applications. Rotello's group used polyamidoamine (PAMAM) dendrimers and AuNPs composites films for the delivery of doxorubicin (DOX).[74] Additionally, these composites are reusable: drug incorporation and release can also be repeated multiple times using the same porous materials.

AuNPs have been considered as prime candidate agents for the photothermal treatment of cancer due to their unique photophysical properties. They overcome limitations of organic-dye-based photothermal agents with low light absorption and undesired photobleaching. Moreover, the antibody or DNA-assisted aggregation of AuNPs on cell membranes or in intracellular environments led to the enhancement of photothermal performances. Wang and coworkers prepared Au supramolecular nanoparticles (Au–SNPs) *via* self-assembly approach. Once RGD incorporating into Au–SNPs, the RGD–Au–SNPs can selectively anchor on U87 glioblastoma cells and come true targeted photothermal treatment of certain types of cancer cells.[75] Recently, Su *et al.* reported that AuNPs-decorated silicon nanowires (AuNPs@SiNWs) can high-efficiently destroy cancer cells within 3 min of near-infrared (NIR) irradiation.[76]

3.3 NanoPCR

The polymerase chain reaction (PCR) is an *in vitro* amplification technology, which became a standard and foremost molecular biological technique with numerous applications in genetic analysis, forensics and *in vitro* diagnostics. Despite great developments, PCR technology is still faced with many challenges, such as low efficiency and specificity. To solve these problems, nanomaterials-assisted PCR (nanoPCR) have received more-and -more attention due to the attractive properties of nanomaterials. For example, we found that AuNPs could significantly improve the specificity of PCR reactions.[77] Later we also reported a new AuNPs-based strategy to dynamically modulate the activity of DNA polymerases and realize a hot start-like PCR with conventional Pfu polymerases.[78]

A PCR-based telomere repeat amplification protocol (TRAP) is the gold-standard assay for detecting the activity of cellular telomerase. However, its use has been significantly limited when performed directly in complex, interferant-laced samples. Inspired by the fact that AuNPs can improve the yield of PCR and reduce non-specific amplification products, Xiao *et al.* improved TRAP assays by using primer-modified AuNPs (Fig. 8).[79] This new assay allows high-fidelity amplification of telomerase products directly from concentrated cell lysates, while traditional TRAP assays do not function effectively in protein-rich clinical samples. This AuNP-based TRAP assay can selectively and readily detect small numbers of cancer cells in extracts containing a large background of telomerase-negative cells (by 2 orders of magnitude excess). In addition, the AuNPs-modified TRAP assay exhibited at least 10-fold higher sensitivity

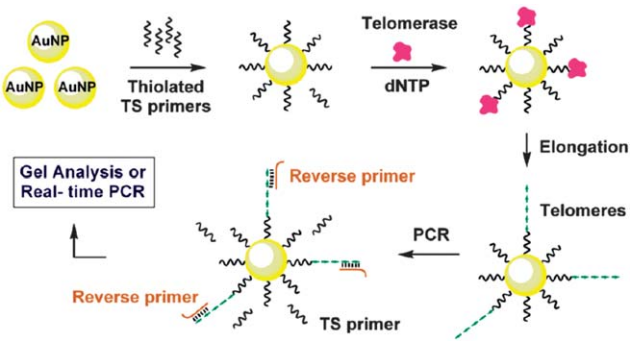

Fig. 8 Schematic illustration of the AuNP-modified trap assay, in which telomere strand (TS) primers covalently attached to AuNPs serve both as substrates for telomerase-induced elongation and templates for subsequent PCR amplification in the same tube. Reprinted from ref. 79 with the permission of American Chemical Society.

than the traditional TRAP assay, which can easily detect the presence of 5 cancer cells doped into 5000 somatic cells.

AuNPs-based nanoPCR is employed not only in telomerase activity,[79,80] DNA, chlamydia infection detection,[81] but also in SNP genotyping and haplotype analysis. The conventional Allele-specific polymerase chain reaction (AS-PCR) is a common technique for SNP genotyping, which can't effectively discriminate DNA mismatches in all situations. Recently, we successfully studied the effects of AuNPs on the ability of AS-PCR to distinguish base mismatches for improving genotyping and haplotyping (Fig. 9).[82] We found that the addition of 1 nm AuNPs significantly increased C_t values for all the mismatched primer/template pairs. In contrast, the fully complementary primer/template pairs were minimally affected by AuNPs. Therefore, AuNPs can selectively inhibit the amplification of mismatched primer/template pairs and enhance the specificity of AS-PCR. As a further step, we also found that AuNPs could be applied in haplotype analysis. This AuNPs-based haplotyping method is scalable and compares favorably with traditional labor-intensive cloning-sequencing methods in both speed and throughput.

3.4 AuNPs-based nanostructures

The programmability of DNA makes it a powerful tool for the rational assembly of nanoparticles into one- two- and three-dimensional arrays. DNA can serve as a directing ligand, controlling the placement of nanoparticles into specific positions within an ordered lattice.[83–85] Assemblies of well-defined AuNPs have attracted much interest because they generate high local-field enhancement when excited at their plasmon resonance, which may inspire new ideas for detectors, optical waveguides, and resonators as well as applications in sensing, spectroscopy, and microscopy. Since Alivisatos' group used DNA mono-modified AuNPs to assemble into dimers and trimers in 1996,[13] DNA–AuNPs conjugates have widely explored in different nanostructures constructions.[1,86,87] For example, DNA–AuNPs conjugates can be selectively attached onto two different hemispheres of DNA-functionalized Janus nanoparticles

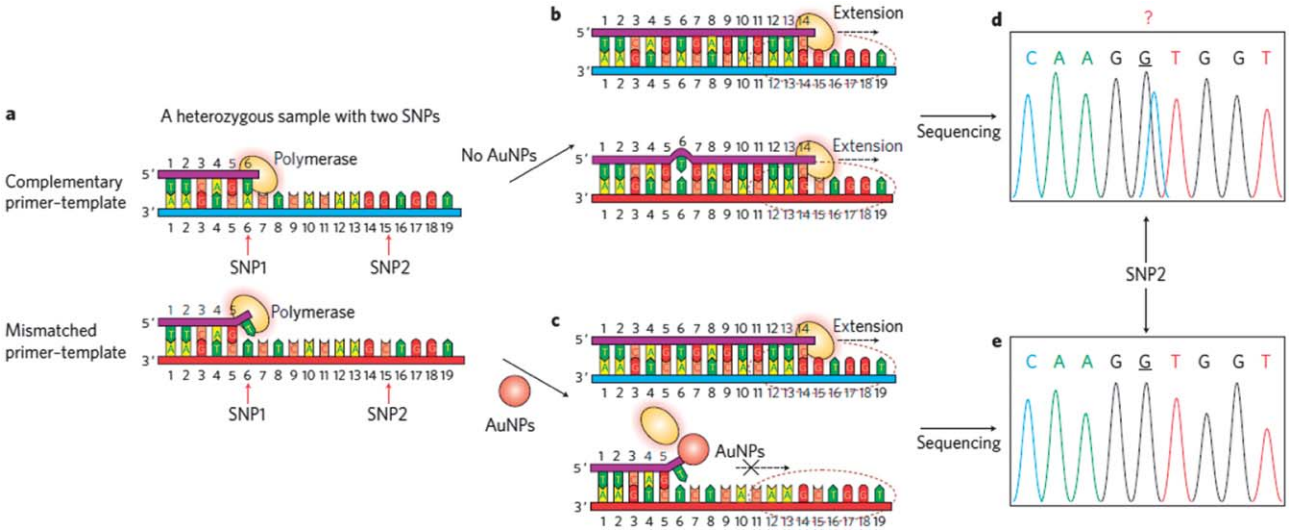

Fig. 9 Schematic showing the AuNPs-enhanced allele-specific sequencing (AuNAS) strategy. A heterozygous sample with two SNPs is amplified with AS-PCR in the presence and absence of AuNPs. The complementary (blue line) and mismatched (red line) template strands are annealed with the allele-specific primers (short purple line). Small polygons with four different colours represent four types of bases (A, yellow; T, green; C, orange; G, red). The two SNP sites are marked with red arrows (SNP1 and SNP2). Yellow oval, polymerase; red circle, AuNPs. Reprinted from ref. 82 with the permission of Nature Publishing Group.

through DNA hybridization, resulting in red shifting of the UV-vis and Plasmon resonance spectra of AuNPs.[88]

DNA–AuNPs conjugates also can be used to assemble into three-dimensional (3D) nanostructures.[1,89] Sharma and coworkers have exhibited various 3D architectures ranging in shape from stacked rings spirals, double spirals, and nested spirals through DNA tubes self-association of multi-helix DNA bundle structures or closing up of 2D DNA tile lattices.[90] As shown in Fig. 10A, a single spiral of 5 nm AuNPs wrapped around a single spiral 10 nm AuNPs (an architecture resembling a double helix) by electron tomographic images. The image shown in Fig. 10B contains a double spiral of 5 nm AuNPs wrapped in double spiral 10 nm AuNPs (an architecture resembling a quadruplex). Ding *et al.* have designed a strategy that uses the scaffold DNA origami method to organize six different-sized AuNPs, which form a linear structure with a well controlled orientation and <10 nm spacing.[91] According to their previous report, Ding and coworkers obtained 3D plasmonic chiral nanostructures through programmable transformation of AuNPs-dressed DNA origami.[92]

DNA–AuNPs conjugates are considered as the basic building blocks that can be rationally assembled through programmable base-pairing interactions into highly ordered macroscopic materials. Park's group designed a series of nanostructures based on DNA functionalized-AuNPs. In 2008, Park *et al.* reported that DNA–AuNPs conjugates can assemble into micrometer-sized face-centred-cubic or body-centred-cubic crystal structures.[93] Their finding offers an opportunity to use single-component system to synthesize directly programmable structures. Recently, Park's group showed the creation of a non-compact lattice by DNA-programmed crystallization using surface-modified Qβ phase capsid particles and AuNPs.[2] As shown in Fig. 11, they combine organic virus-like protein nanoparticles (VLPs) and inorganic AuNPs to form NaTl-type colloidal crystalline structure through the proper connecting oligonucleotides. The ability to use both nanoparticles and DNA base pairing interactions to assemble sophisticated nanostructures with such diverse properties opens the door to new and exciting possibilities for colloidal crystallization and materials assembly. More recently, Mirkin's group used

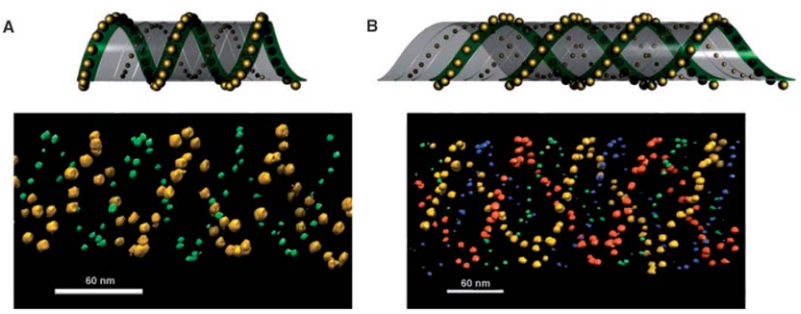

Fig. 10 The tubes formed with 5 and 10 nm AuNPs placed on opposite surfaces of the DNA tile array. (A and B) The top panels are schematic side and top views of the binary particle tube architectures; the bottom panels are corresponding representative electron tomographic images clearly showing the 3D architectures. Reprinted from ref. 90 with the permission of American Association for the advancement of Science.

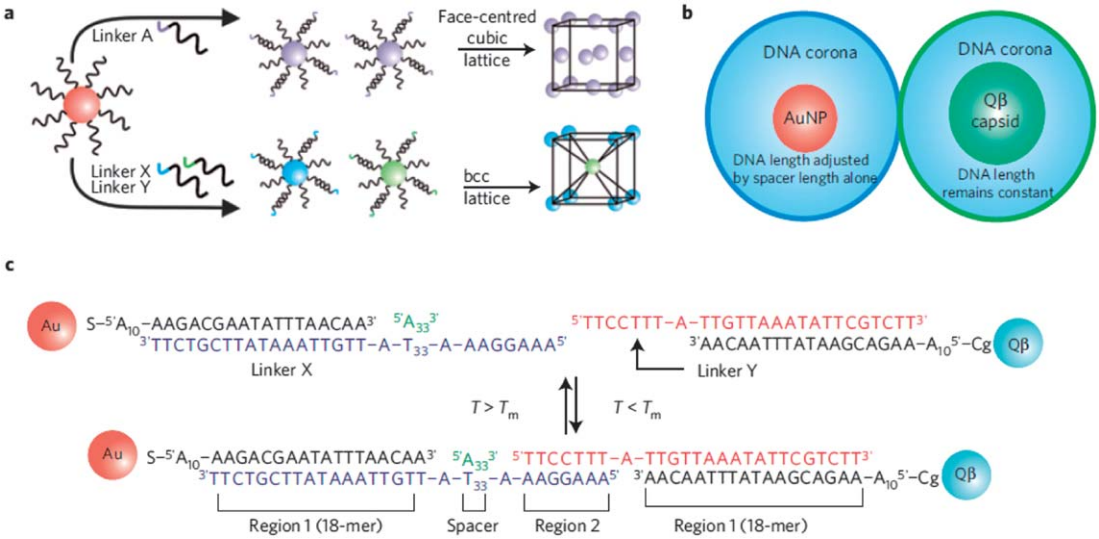

Fig. 11 DNA-programmable nanoparticle crystallization method. (a) Different crystallographic arrangements can be programmed by changing the terminal part of the DNA linker sequence. (b) Matching the effective radii of DNA-linked particles by adjusting the length of the spacer DNA linker to compensate for changes in the Au core particle diameter. Dark rings around DNA coronas indicate the sticky ends of linkers X and Y. (c) Details of the binary-component assembly system in which AuNPs and VLPs are assembled using two different DNA linkers-X and Y. Reprinted from ref. 2 with the permission of Nature Publishing Group.

"three-dimensional spacers" within nanoparticle superlattices to assemble hollow DNA nanostructures *via* programmable DNA interactions.[94]

Conclusion

The wide range of surface functionality and bioconjugates, coupled with the outstanding physical properties of AuNPs ensures their successful application in many chemical and biological fields. AuNPs have been considered as promising multicomponent nanocarriers with a high surface-to-volume ratio, which exhibit high sensitivity and selectivity for the simultaneous detection of multianalytes. Moreover, the tunable synthesis approaches and almost limitless chemical or biological functional groups make it a hot nanomaterial for controllable drug delivery and therapy. We also envision that the applications of AuNPs in PCR and other biological systems may eventually lead to a new era of bionanotechnology.

Notes and references

1 T. Zhang, Z. Yang and D. S. Liu, *Nanoscale*, 2011, **3**, 4015–4021.
2 P. Cigler, A. K. R. Lytton-Jean, D. G. Anderson, M. Finn and S. Y. Park, *Nat. Mater.*, 2010, **9**, 918–922.
3 M. C. Daniel and D. Astruc, *Chem. Rev.*, 2004, **104**, 293–346.
4 D. T. Thompson, *Nano Today*, 2007, **2**, 40–43.
5 K. Saha, S. S. Agasti, C. Kim, X. Li and V. M. Rotello, *Chem. Rev.*, 2012, **112**, 2739.
6 S. P. Song, Y. Qin, Y. He, Q. Huang, C. H. Fan and H. Y. Chen, *Chem. Soc. Rev.*, 2010, **39**, 4234–4243.
7 D. Liu, Z. Wang and X. Jiang, *Nanoscale*, 2011, **3**, 1421–1433.
8 S. Rana, A. Bajaj, R. Mout and V. M. Rotello, *Adv. Drug Delivery Rev.*, 2012, **64**, 200–216.
9 D. A. Giljohann, D. S. Seferos, W. L. Daniel, M. D. Massich, P. C. Patel and C. A. Mirkin, *Angew. Chem., Int. Ed.*, 2010, **49**, 3280–3294.
10 E. C. Dreaden, A. M. Alkilany, X. Huang, C. J. Murphy and M. A. El-Sayed, *Chem. Soc. Rev.*, 2012, **41**, 2740–2779.
11 L. Zhang, Y. Li, D. W. Li, C. Jing, X. Chen, M. Lv, Q. Huang, Y. T. Long and I. Willner, *Angew. Chem.*, 2011, **123**, 6921–6924.
12 Z. Z. J. Lim, J. E. J. Li, C. T. Ng, L. Y. L. Yung and B. H. Bay, *Acta Pharmacol. Sin.*, 2011, **32**, 983–990.
13 A. P. Alivisatos, K. P. Johnsson, X. Peng, T. E. Wilson, C. J. Loweth, M. P. Bruchez and P. G. Schultz, *Nature*, 1996, **382**, 609–611.
14 C. A. Mirkin, R. L. Letsinger, R. C. Mucic and J. J. Storhoff, *Nature*, 1996, **382**, 607–609.
15 A. K. R. Lytton-Jean, R. Langer and D. G. Anderson, *Small*, 2011, **7**, 1932–1937.
16 R. Arvizo, R. Bhattacharya and P. Mukherjee, *Expert Opin. Drug Delivery*, 2010, **7**, 753–763.
17 J. Turkevich, P. C. Stevenson and J. Hillier, *Discuss. Faraday Soc.*, 1951, **11**, 55–75.
18 A. Zaki, N. Dave and J. Liu, *J. Am. Chem. Soc.*, 2012, **134**, 35–38.
19 X. Zhang, M. R. Servos and J. W. Liu, *J. Am. Chem. Soc.*, 2012, **134**, 9910–9913.
20 C. Vericat, M. Vela, G. Benitez, P. Carro and R. Salvarezza, *Chem. Soc. Rev.*, 2010, **39**, 1805–1834.
21 M. Kanehara, J. Sakurai, H. Sugimura and T. Teranishi, *J. Am. Chem. Soc.*, 2009, **131**, 1630–1631.
22 J. J. Storhoff, A. A. Lazarides, R. C. Mucic, C. A. Mirkin, R. L. Letsinger and G. C. Schatz, *J. Am. Chem. Soc.*, 2000, **122**, 4640–4650.
23 S. J. Hurst, A. K. R. Lytton-Jean and C. A. Mirkin, *Anal. Chem.*, 2006, **78**, 8313–8318.

24 X. Zhang, M. R. Servos and J. W. Liu, *J. Am. Chem. Soc.*, 2012, **134**, 7266–7269.
25 N. Bhatt, P. J. J. Huang, N. Dave and J. Liu, *Langmuir*, 2011, **27**, 6132–6137.
26 L. M. Demers, M. Östblom, H. Zhang, N. H. Jang, B. Liedberg and C. A. Mirkin, *J. Am. Chem. Soc.*, 2002, **124**, 11248–11249.
27 A. Opdahl, D. Y. Petrovykh, H. Kimura-Suda, M. J. Tarlov and L. J. Whitman, *Proc. Natl. Acad. Sci. U. S. A.*, 2007, **104**, 9–14.
28 S. M. Schreiner, D. F. Shudy, A. L. Hatch, A. Opdahl, L. J. Whitman and D. Y. Petrovykh, *Anal. Chem.*, 2010, **82**, 2803–2810.
29 S. M. Schreiner, A. L. Hatch, D. F. Shudy, D. R. Howard, C. Howell, J. Zhao, P. Koelsch, M. Zharnikov, D. Y. Petrovykh and A. Opdahl, *Anal. Chem.*, 2011, **83**, 4288–4295.
30 H. Pei, F. Li, Y. Wan, M. Wei, H. Liu, Y. Su, N. Chen, Q. Huang and C. H. Fan, *J. Am. Chem. Soc.*, 2012, **134**, 11876–11879.
31 E. Katz and I. Willner, *Angew. Chem., Int. Ed.*, 2004, **43**, 6042–6108.
32 D. Tang, J. Tang, B. Su and G. Chen, *Biosens. Bioelectron.*, 2011, **26**, 2090–2096.
33 V. Aina, T. Marchis, E. Laurenti, E. Diana, G. Lusvardi, G. Malavasi, L. Menabue, G. Cerrato and C. Morterra, *Langmuir*, 2010, **26**, 18600–18605.
34 V. Chegel, O. Rachkov, A. Lopatynskyi, S. Ishihara, I. Yanchuk, Y. Nemoto, J. P. Hill and K. Ariga, *J. Phys. Chem. C*, 2012, **116**, 2683–2690.
35 A. Laforgue, T. Addou and D. Bélanger, *Langmuir*, 2005, **21**, 6855–6865.
36 M. G. Paulik, P. A. Brooksby, D. Andrew and A. J. Downard, *J. Phys. Chem. C*, 2007, **111**, 7808–7815.
37 D. M. Shewchuk and M. T. McDermott, *Langmuir*, 2009, **25**, 4556–4563.
38 L. Laurentius, S. R. Stoyanov, S. Gusarov, A. Kovalenko, R. Du, G. P. Lopinski and M. T. McDermott, *ACS Nano*, 2011, **5**, 4219–4227.
39 X. Zhou, S. J. Xia, Z. Q. Lu, Y. Tian, Y. S. Yan and J. Zhu, *J. Am. Chem. Soc.*, 2010, **132**, 6932–6934.
40 F. Xia, X. Zuo, R. Yang, Y. Xiao, D. Kang, A. Vallée-Bélisle, X. Gong, J. D. Yuen, B. B. Y. Hsu and A. J. Heeger, *Proc. Natl. Acad. Sci. U. S. A.*, 2010, **107**, 10837.
41 A. Faccenda, C. A. Bonham, P. O. Vacratsis, X. Zhang and B. Mutus, *J. Am. Chem. Soc.*, 2010, **132**, 11392–11394.
42 J. Yan, S. P. Song, B. Li, Q. Zhang, Q. Huang, H. Zhang and C. H. Fan, *Small*, 2010, **6**, 2520–2525.
43 A. Bonanni, M. Pividori and M. Del Valle, *Analyst*, 2010, **135**, 1765–1772.
44 S. Liu, P. Wu, W. Li, H. Zhang and C. X. Cai, *Anal. Chem.*, 2011, **83**, 4752–4758.
45 C. Y. Lin, C. J. Yu, Y. H. Lin and W. L. Tseng, *Anal. Chem.*, 2010, **82**, 6830–6837.
46 D. Liu, W. Qu, W. Chen, W. Zhang, Z. Wang and X. Jiang, *Anal. Chem.*, 2010, **82**, 9606–9610.
47 D. Liu, W. Chen, K. Sun, K. Deng, W. Zhang, Z. Wang and X. Jiang, *Angew. Chem., Int. Ed.*, 2011, **50**, 4103–4107.
48 J. Zhang, L. Wang, H. Zhang, F. Boey, S. P. Song and C. H. Fan, *Small*, 2010, **6**, 201–204.
49 N. H. Kim, S. J. Lee and M. Moskovits, *Adv. Mater.*, 2011, **23**, 4152–4156.
50 M. Comotti, C. Della Pina, R. Matarrese and M. Rossi, *Angew. Chem., Int. Ed.*, 2004, **43**, 5812–5815.
51 W. J. Luo, C. F. Zhu, S. Su, D. Li, Y. He, Q. Huang and C. H. Fan, *ACS Nano*, 2010, **4**, 7451–7458.
52 X. Zheng, Q. Liu, C. Jing, Y. Li, D. Li, W. Luo, Y. Wen, Y. He, Q. Huang and Y. T. Long, *Angew. Chem.*, 2011, **123**, 12200–12204.
53 K. K. Maiti, A. Samanta, M. Vendrell, K.-S. Soh, M. Olivo and Y.-T. Chang, *Chem. Commun.*, 2011, **47**, 3514–3516.
54 K. Lee, H. Lee, K. H. Bae and T. G. Park, *Biomaterials*, 2010, **31**, 6530–6536.
55 O. R. Miranda, X. Li, L. Garcia-Gonzalez, Z. J. Zhu, B. Yan, U. H. F. Bunz and V. M. Rotello, *J. Am. Chem. Soc.*, 2011, **133**, 9650–9653.
56 Y. Jiang, H. Zhao, Y. Lin, N. Zhu, Y. Ma and L. Q. Mao, *Angew. Chem.*, 2010, **122**, 4910–4914.
57 C. Wang, J. Chen, T. Talavage and J. Irudayaraj, *Angew. Chem.*, 2009, **121**, 2797–2801.
58 K. Cheng, S. Peng, C. Xu and S. Sun, *J. Am. Chem. Soc.*, 2009, **131**, 10637.
59 A. A. Bhirde, V. Patel, J. Gavard, G. Zhang, A. A. Sousa, A. Masedunskas, R. D. Leapman, R. Weigert, J. S. Gutkind and J. F. Rusling, *ACS Nano*, 2009, **3**, 307–316.
60 K. Kostarelos, A. Bianco and M. Prato, *Nat. Nanotechnol.*, 2009, **4**, 627–633.
61 C. M. Alexander, M. M. Maye and J. C. Dabrowiak, *Chem. Commun.*, 2011, **47**, 3418–3420.
62 C. M. Alexander, J. C. Dabrowiak and M. M. Maye, *Bioconjugate Chem.*, 2012, **23**, 2061–2070.
63 S. D. Brown, P. Nativo, J. A. Smith, D. Stirling, P. R. Edwards, B. Venugopal, D. J. Flint, J. A. Plumb, D. Graham and N. J. Wheate, *J. Am. Chem. Soc.*, 2010, **132**, 4678–4684.
64 X. Wang, L. Yang, Z. G. Chen and D. M. Shin, *Ca-Cancer J. Clin.*, 2008, **58**, 97–110.
65 G. F. Paciotti, D. G. I. Kingston and L. Tamarkin, *Drug Dev. Res.*, 2006, **67**, 47–54.
66 S. Jelveh and D. B. Chithrani, *Cancers*, 2011, **3**, 1081–1110.
67 A. S. Thakor, J. Jokerst, C. Zavaleta, T. F. Massoud and S. S. Gambhir, *Nano Lett.*, 2011, **11**, 4029–4036.
68 L. Maus, O. Dick, H. Bading, J. P. Spatz and R. Fiammengo, *ACS Nano*, 2010, **4**, 6617–6628.
69 S. Bhattacharyya, R. D. Singh, R. Pagano, J. D. Robertson, R. Bhattacharya and P. Mukherjee, *Angew. Chem., Int. Ed.*, 2012, **51**, 1563–1567.
70 B. Kim, G. Han, B. J. Toley, C. Kim, V. M. Rotello and N. S. Forbes, *Nat. Nanotechnol.*, 2010, **5**, 465–472.
71 C. Kim, S. S. Agasti, Z. Zhu, L. Isaacs and V. M. Rotello, *Nat. Chem.*, 2010, **2**, 962–966.
72 C. E. Ashley, E. C. Carnes, G. K. Phillips, D. Padilla, P. N. Durfee, P. A. Brown, T. N. Hanna, J. Liu, B. Phillips and M. B. Carter, *Nat. Mater.*, 2011, **10**, 389–397.
73 J. B. Song, J. J. Zhou and H. W. Duan, *J. Am. Chem. Soc.*, 2012, **134**, 13458–13469.
74 M. H. Park, S. S. Agasti, B. Creran, C. Kim and V. M. Rotello, *Adv. Mater.*, 2011, **23**, 2839–2842.

75 S. Wang, K. J. Chen, T. H. Wu, H. Wang, W. Y. Lin, M. Ohashi, P. Y. Chiou and H. R. Tseng, *Angew. Chem., Int. Ed.*, 2010, **49**, 3777–3781.
76 Y. Y. Su, X. P. Wei, F. Peng, Y. L. Zhong, Y. M. Lu, S. Su, T. T. Xu, S. T. Lee and Y. He, *Nano Lett.*, 2012, **12**, 1845–1850.
77 H. K. Li, J. H. Huang, J. H. Lv, H. J. An, X. D. Zhang, Z. Z. Zhang, C. H. Fan and J. Hu, *Angew. Chem., Int. Ed.*, 2005, **44**, 5100–5103.
78 L. J. Mi, Y. Q. Wen, D. Pan, Y. H. Wang, C. H. Fan and J. Hu, *Small*, 2009, **5**, 2597–2600.
79 Y. Xiao, K. Y. Dane, T. Uzawa, A. Csordas, J. Qian, H. T. Soh, P. S. Daugherty, E. T. Lagally, A. J. Heeger and K. W. Plaxco, *J. Am. Chem. Soc.*, 2010, **132**, 15299–15307.
80 J. S. Wang, L. Wu, J. S. Ren and X. G. Qu, *Small*, 2012, **8**, 259–364.
81 Y. L. Jung, C. Jung, H. Parab, T. Li and H. G. Park, *Biosens. Bioelectron.*, 2010, **25**, 1941–1946.
82 P. Chen, D. Pan, C. H. Fan, J. Chen, K. Huang, D. Wang, H. Zhang, Y. Li, G. Feng and P. Liang, *Nat. Nanotechnol.*, 2011, **6**, 639–644.
83 H. Gu, J. Chao, S. J. Xiao and N. C. Seeman, *Nature*, 2010, **465**, 202–205.
84 S. J. Tan, M. J. Campolongo, D. Luo and W. Cheng, *Nat. Nanotechnol.*, 2011, **6**, 268–276.
85 D. Sun and O. Gang, *J. Am. Chem. Soc.*, 2011, **133**, 5252–5254.
86 C. H. Lalander, Y. Zheng, S. Dhuey, S. Cabrini and U. Bach, *ACS Nano*, 2010, **4**, 6153–6161.
87 T. J. Song and H. J. Liang, *J. Am. Chem. Soc.*, 2012, **134**, 10803–10806.
88 H. Xing, Z. Wang, Z. Xu, N. Y. Wong, Y. Xiang, G. L. Liu and Y. Lu, *ACS Nano*, 2012, **6**, 802–809.
89 Y. H. Roh, R. C. H. Ruiz, S. Peng, J. B. Lee and D. Luo, *Chem. Soc. Rev.*, 2011, **40**, 5730–5744.
90 J. Sharma, R. Chhabra, A. Cheng, J. Brownell, Y. Liu and H. Yan, *Science*, 2009, **323**, 112–116.
91 B. Ding, Z. Deng, H. Yan, S. Cabrini, R. N. Zuckermann and J. Bokor, *J. Am. Chem. Soc.*, 2010, **132**, 3248–3249.
92 X. Shen, C. Song, J. Wang, D. Shi, Z. Wang, N. Liu and B. Ding, *J. Am. Chem. Soc.*, 2012, **134**, 146–149.
93 S. Y. Park, A. K. R. Lytton-Jean, B. Lee, S. n. Weigand, G. C. Schatz and C. A. Mirkin, *Nature*, 2008, **451**, 553–556.
94 E. Auyeung, J. I. Cuter, R. J. Macfarlane, M. R. Jones, J. S. Wu, G. Liu, K. Zhang, K. D. Osberg and C. A. Mirkin, *Nat. Nanotechnol.*, 2012, **7**, 24–28.